In: *Structure and Dynamics of Earth's Deep Interior*, D.E. Smylie and R. Hide Editors, *Amer. Geophys. Un., Geophys. Monog.*, 46, pp. 55-63, 1988.

EVIDENCE FOR LATERAL HETEROGENEITY AT THE CORE-MANTLE BOUNDARY FROM THE SLOWNESS OF DIFFRACTED S PROFILES

Michael E. Wysession and Emile A. Okal

Department of Geological Sciences, Northwestern University, Evanston, Illinois 60208

Abstract. A regional study of SH velocities in D" has been conducted through the comparison of the apparent ray parameters of diffracted SH waves [*Sd*] from large earthquakes and synthetic pulses generated by normal mode summation for three different velocity structures. This technique has the advantage of automatically including all non-geometric optics effects in the calculation of the synthetics and of avoiding the complications due to varying waveform frequency content that arise when trying to directly convert apparent slownesses into mantle velocities.

We computed the excitation functions of torsional normal modes up to 0.05 Hz for the smooth model PREM, a model PREM(HVZ) incorporating Lay and Helmberger's [1983a] proposed high-velocity zone, and a PREM(LVZ) low-velocity structure. The apparent slownesses for the path profiles were obtained by cross-correlations of both the synthetic *Sd* arrivals, corrected for ellipticity using the modal approximations of Dahlen [1975], and the data, which were filtered and corrected for upper mantle heterogeneity (using the tomographic SH velocity models of Woodhouse and Dziewonski [1983], and Tanimoto [1987] so as to be compatible with the synthetics). Comparisons of the cross-correlated slownesses revealed one region on the CMB with D" velocities slower than those of PREM, one region compatible with PREM, two zones distinctly faster than PREM and one zone that strongly represents a region of high velocity. This high-velocity zone was also identified as such by the Lay and Helmberger [1983a] study.

Introduction

The structure and dynamics of the so-called D" region at the base of the mantle have continued over the past two decades to arouse much interest and controversy among a variety of disciplines. Most early models of the shear velocity above the core-mantle boundary (CMB) displayed a homogeneous low velocity zone [Cleary, 1969; Hales and Roberts, 1970; Bolt et al., 1970], which is consistent with the concept of D" as a simple thermal boundary layer [Jeanloz and Richter, 1979]; later models suggested heterogeneous regions of low velocity [Bolt and Niazi, 1984]. However, subsequent studies have presented a wider variety of models, some with high velocity zones in D" [Mitchell and Helmberger, 1973; Mula and Müller, 1980; Lay and Helmberger, 1983], and recent work by several authors has found evidence for large scale heterogeneity at the base of the mantle [Gudmundsson et al., 1986; Woodhouse and Dziewonski, 1987]. The determination of the seismic velocities in D" is of great importance in discerning the dynamic processes at work along the CMB. The average values of the seismic velocities should provide insight into the general thermal and mineralogical structure of D", while lateral heterogeneity may help map areas of upward convection (expected to feature low velocities and low-Q) and, conversely, zones of sinking of colder convected mantle (expected to be faster), as suggested, for example, by Olson et al. [1987].

While studies of D" have utilized a wide range of techniques, we concentrate in this paper on the determination of the apparent slowness of diffracted S [hereafter *Sd*] arrivals (Figure 1). We are motivated to a large extent by the results of Lay and Helmberger [1983a], who interpreted teleseismic S arrivals in the distance range 75—90° as triplications due to a zone of high S velocities approximately 280 km thick and 2.75% fast. If confirmed, such a structure would have important implications for the structure and mineralogy of D". These authors' interpretation was however non-unique, since the later arrivals making up the triplication could be due to near-source heterogeneity or the effect of scattering along the CMB. A summary of these arguments and of the ensuing controversy can be found in Schlittenhardt et al. [1985], Haddon and Buchbinder [1986] and Lay [1986].

Difficulties with *Sd* Ray Parameters

The use of a profile of diffracted S waves leaving the source at a common azimuth should in principle alleviate this problem, since the downswing part of the path from the source to the core is common to all rays in the profile, and near-source complexity cancels out of the apparent slowness. We refer to Okal and Geller [1979], Mula and Müller [1980], and Bolt and Niazi [1984] for previous work on *Sd*; in general, these studies successfully measured the slowness $p = dT/d\Delta$ of the wave along a profile of stations. As pointed out for example by Aki and Richards [1980], the interpretation of p in terms of the shear-wave velocity at the CMB is not simple because the diffracted arrivals, in violation of the laws of geometrical optics, propagate along the CMB with varying frequencies travelling through varying depths into D", the longer wavelengths of the lower frequencies sampling further up into the mantle. This causes complications in several manners: (1) for a D" model featuring a velocity gradient, dispersion of the diffracted ray will occur with different frequencies travelling through regions of different velocity; (2) as the ray propagates along the CMB, its amplitude decreases (due to diffraction back into the mantle) as $\exp[-a\,\omega^{1/3}\Delta]$, where Δ is distance along the CMB and ω angular frequency [Aki and Richards, 1980, p. 440]; (3) anelastic attenuation further reduces the high frequency components of the signal.

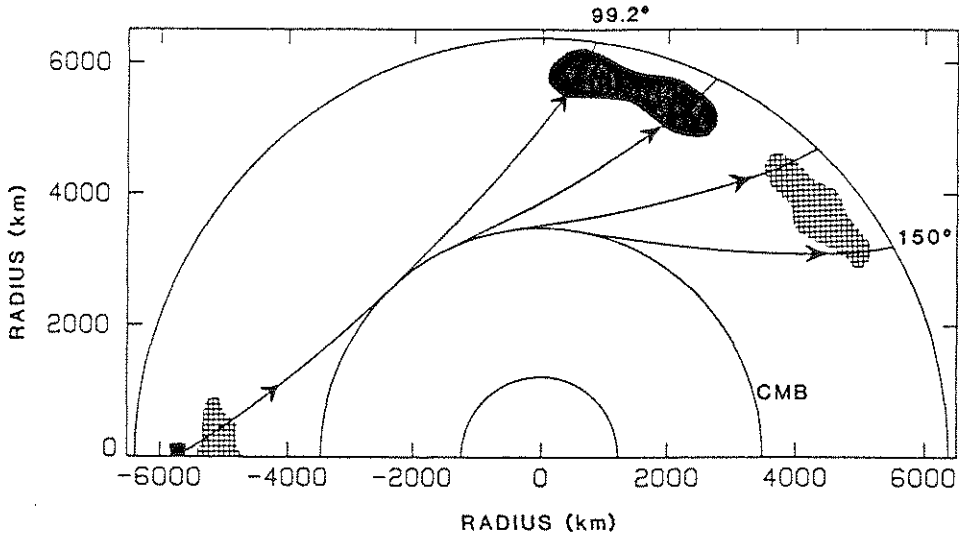

Fig. 1. Sketch of the path of four diffracted S (*Sd*) waves from a 600 km deep earthquake, generated for a PREM earth [*Dziewonski and Anderson*, 1981]. On a geometric basis the first *Sd* arrivals would appear after 99.2°, and the phase is found beyond 150°. The downswing paths are not differentiated by mantle heterogeneity, which is not the case for the *Sd* upswing paths.

As a result, each arrival with a different epicentral distance will have a different waveform due to its varying frequency content [Chapman and Phinney, 1972]. This is particularly important because it means that the value of the slowness obtained from cross-correlation along a particular path will be dependent upon the relative locations of the stations, and one would expect the slowness along a given portion of the CMB to vary with the addition and removal of stations. Mula and Müller [1980] recognized this problem and found that the apparent ray parameter varied with different dominant frequencies for synthetic seismograms computed by the reflectivity method. The value of the slowness will also depend upon the technique used in measuring the trend, and all methods will be arbitrary to some degree as they are subject to the varying frequency content of the arrivals.

For these reasons, in the present paper, we retrieve only the slowness from the data, and use forward modeling to determine an appropriate D" velocity structure by generating synthetic *Sd* waves from a given initial velocity model and comparing the synthetics' slowness with that of the data. An initial velocity model is deemed appropriate only to the extent of the similarity between the two slownesses. The synthetics are computed by normal mode theory, which has the advantage of including all diffraction effects automatically [Okal, 1978].

While the ray parameter from a set of *Sd* waves is, to the first order, the linear trend of the successive arrivals at increasing distances along the CMB, there are several factors which must be corrected or accounted for. It is very important, for example, that a narrow azimuthal range be accepted in the inclusion of arrivals for a given path. Recent work by Cormier [1987] has shown that contamination of *S* rays by slab-diffracted energy can cause a difference in arrival times of several seconds for rays leaving an event at different azimuths. In addition, rays at varying azimuths could accrue travel-time differences due to their different downswing paths through the heterogeneous mantle. A narrow azimuthal range not only eliminates errors due to source effects and downswing heterogeneity but also allows the rays to sample the same portions of the CMB.

A problem which has not been addressed in previous studies of diffracted ray slownesses has been the effect of ellipticity. This effect, though usually not large, is variable depending upon the azimuth of a profile and the distribution of stations along it. For example, in a set of *Sd* arrivals starting at high latitudes and approaching the equator, successive arrivals would travel increasingly greater distances through the mantle, causing a bias toward a larger ray parameter and therefore erroneously implying a D" low velocity zone. We have corrected for the ellipticity by including modal approximation terms in the generation of our synthetic seismograms.

Finally, a problem that previous *Sd* studies have not been able to correct for is the differing *Sd* upswing paths, seen in Figure 1. Diffracted S waves can arrive over a wide distance range, often causing the upswing paths to rise through different regions of the notoriously heterogeneous upper mantle, even for rays leaving a single event with the same azimuth. If, for example, the closest *Sd* arrivals are through a fast continental shield region and the furthest rays come up through a slow young oceanic structure, the trend through the arrivals would be biased towards a larger ray parameter value and again would falsely imply a D" low velocity zone. We address this problem by using available models of upper mantle lateral heterogeneity to compute travel-time corrections over all upswing paths, before computing the experimental slowness for each profile. The resulting corrections are significant along certain profiles.

Data and Analysis

A total of 71 *Sd* arrivals were used from 38 WWSSN and Canadian (and the Palisades Press-Ewing) stations, allowing the determination of ray parameters for 12 paths along 5 different regions of the CMB. Both horizontal components were digitized, interpolated at 0.5 s intervals using a cubic polynomial scheme and rotated into their transverse components. In the PREM model [Dziewonski and Anderson, 1981] the calculated first *Sd* rays arrive at epicentral distances of $\Delta = 99.2°$ for an event at 600 km

TABLE 1. Earthquakes Used in This Study

No.	Region	Date	Origin Time	Depth (km)	Epicenter °N	Epicenter °E	m_b	Focal Mechanism ϕ	δ	λ	Ref.
1	New Guinea	4/24/64	05:56:09.8	99	-5.07	144.20	6.3	183	80	-90	a
2	Loyalty Is.	10/7/66	15:55:11.3	165	-21.59	170.56	6.0	107	70	21	a
3	Tonga	10/9/67	17:21:46.0	605	-21.10	-179.20	6.2	54	85	-83	a
4	Tonga	2/10/69	22:58:03.3	635	-22.75	178.76	6.0	96	86	-65	b
5	Burma	7/29/70	10:16:20.4	68	26.02	95.37	6.4	197	60	165	c
6	Kuril Is.	1/29/71	21:58:05.4	515	51.69	150.97	6.0	35	71	-90	d
7	Tonga	11/20/71	07:27:59.5	533	-23.45	-179.88	6.0	160	75	100	d
8	Tonga	2/22/75	22:04:33.5	333	-24.98	-178.88	6.1	35	87	-143	d
9	Honshu	6/29/75	10:37:40.6	549	38.79	130.09	6.1	222	78	120	d
10	Honshu	3/9/77	14:27:53.6	579	41.61	130.88	5.9	194	75	76	e

References for focal mechanisms: a= *Isacks and Molnar* [1971]; b= *Mula* [1981]; c= *Tandon and Srivastava* [1975]; d= This study; e= *Giardini* [1984].

depth, and $\Delta = 101.6°$ for a surface event, so we tried to avoid using any arrivals closer than 100°, only twice using rays that could contain mostly undiffracted S energy. The SH energy decays quickly along the CMB, but we found as appropriate for the study four of the Sd arrivals recorded beyond 150°, making the range of the CMB sampled by a given profile to be as large as 50°, or approximately 3000 km. It was always our attempt to get as many arrivals with as wide a distance range as possible for each path used. While there is most probably inhomogeneity in D" on scale smaller than 3000 km, and a slowness retrieved over this nge will be a large scale average, this trade-off was propitious due to the more precise determination of the ray parameter using a broader distance range. Tables 1 and 2 list epicentral and path information for the records used in this study.

In order to retain large amounts of SH energy around the CMB, the events used in this study, all with $m_b > 5.9$, involved predominantly dip-slip motion as can be seen from the focal mechanisms listed in Table 1. The source parameters were either taken from previous studies or calculated on the basis of first arrivals that were both read directly from the data and taken from ISC bulletins. We tried to use primarily deep events for several reasons. First, the LVZ at the base of the lithosphere greatly attenuates S waves that pass through it, and rays from deeper events pass through this zone once instead of twice. The two earthquakes we used that were shallower than 100 km also happened to have the two greatest body magnitudes ($m_b = 6.3$ and 6.4). Records from deep events are usually cleaner and less noisy, making the Sd arrivals more distinct, but more importantly with deep events Sd is also distinct from the surface reflected sSd, simplifying the procedure to determine the slowness. Only in the case of Event 5, were Sd and sSd too close to be separated in the cross-correlation process, the consequences of which are discussed later.

Another requirement for the earthquake sources was that their SH radiation patterns be favorable for the azimuths along which a string of stations were located. The allowed range in azimuths from a given event to individual stations was usually limited to 10°, so the geographical locations of existing stations and large seismic events not only limited the CMB paths we could study but also forced us to use events with large relative radiation amplitudes. These can be calculated following Kanamori and Stewart [1976] as $R^{SH} = -q_L \cos i_h - p_L \sin i_h$, where q_L and p_L are the

TABLE 2. Characteristics of the Sd Profiles Used in This Study

No.	Ave. Azimuth (°)	R^{SH}	Stations used
1	335.5	0.831	NUR, KON, ESK, VAL, PTO
2	295.5	0.481	NDI, LAH, QUE, MSH, SHI, JER
3a	51.5	0.920	FLO, SCP, PAL, WES, HAL, STJ, PDA
3b	292.0	0.458	SHL, NDI, QUE, SHI
4a	54.0	0.566	OXF, AAM, BLA, SCB, SCP, GEO, OGD, STJ
4b	294.0	0.593	NDI, KBL, MSH, SHI, TAB, JER, HLW
5	0.0	0.230	AAM, SCP, FLO, BLA, OXF, ATL, SHA
6	55.5	0.754	BOG, QUI, NNA, ARE, LPB
7	291.0	0.589	NDI, QUE, SHI, JER, EIL
8	54.0	0.288	OXF, AAM, BLA, SCP, WES, STJ
9	35.5	0.506	ATL, SHA, BHP, BOG, QUI, LPB
10	32.5	0.712	ATL, SHA, CAR, BOG, LPB

radiation-pattern coefficients of Kanamori and Cipar [1974], and i_h is the take-off angle at the focal sphere, which here ranged from $i_h = 19.9°$ (at 68 km depth) to $i_h = 27.6°$ (at 635 km depth). With the optimal relative amplitude as $R^{SH} = 1$, at the azimuths of our profiles all of the events had values of $R^{SH} > 0.4$ with the exception of Events 5 ($R^{SH} = 0.23$) and 8 ($R^{SH} = 0.29$), which were retained because of their clear arrivals.

Finally, the data profiles were filtered with a low-pass filter of 0.05 Hz to make them compatible with the synthetic profiles. Figure 2 shows an example of *Sd* profile in the case of Event 4.

Upper Mantle Corrections

In order to further equate the filtered data with the synthetics, corrections for upper mantle heterogeneity along the *Sd* upswings were added to the travel times based on the tomographic full-mantle shear velocity model of Woodhouse [personal communication, 1987]. The upper mantle model of Tanimoto [1987] was also used, without significant differences.

The corrections were simply computed as

$$\Delta t = -\int_{\text{upswing}} \frac{\Delta\beta}{\beta^2}\, ds \qquad (1)$$

where the integral is taken along the upswing portion of the ray, and the lateral heterogeneity in shear velocity, $\Delta\beta$, is computed locally by summing its spherical harmonics components.

The range in arrival corrections to our data was 2.41 s ($\Delta t = -1.83$ s for Event 4 to SCB; $\Delta t = 0.58$ s for Event 2 to HLW). The greatest range in travel-time corrections for a single profile was 1.53 s (Event 4 to N. America), and the resulting slownesses reflect these biases.

Synthetic Seismograms and Ellipticity Corrections

Since the D" velocity structure cannot be directly inferred from the data ray parameters, synthetic seismograms for three different velocity models were used as a standard of comparison. The synthetics were generated using a summation of toroidal normal modes of free earth oscillations with the algorithm of Kanamori and Cipar [1974], and corrected for ellipticity using the modal approximations of Dahlen [1975]. This method has the advantage of being able to replicate diffracted SH arrivals, which as non-geometrical rays are not well modeled by some other techniques. For each velocity model the excitation functions with depth of almost 7000 modes (with frequencies up to 0.05 Hz and phase velocities above 8.0 km/s) were generated, and each synthetic seismogram was obtained by the summation of the modes; computational details can be found in Okal [1978]. The synthetics for each event were generated using the appropriate focal mechanisms listed in Table 1. As can be seen in Figure 2, using such a broad range of modes generates not only the diffracted *S* rays, but a complete set of SH body wave arrivals.

Velocity Models

The three velocity models used in creating the synthetics typify the types of models that have been invoked by many studies of D"; they are shown on Figure 3. All three of our models have a PREM structure down to a radius of 4075 km and have a CMB at $r = 3480$ km, but while one maintains the PREM values down to the CMB, the other two are perturbed to include high-velocity and low-velocity zones at the base of the mantle. The undisturbed PREM model, based on free earth oscillation data, is used to represent models having zero or small velocity gradients in D", actually including a very small negative gradient of -8.42×10^{-5} s^{-1} in the bottom 70 km and reaching a shear velocity of 7.2254 km/s at the CMB.

The HVZ model is in the manner of Lay and Helmberger [1983a], where evidence for a high-velocity zone was inferred from D" triplication patterns, and consists of 280 km of faster material reaching a maximum of 7.281 km/s at the CMB. Consistent with its initial design, this HVZ is discontinuously separated from a

TABLE 3. Cross-correlated Slownesses (s/deg)

Path Number	Region Sampled	Observed slowness		Synthetic slowness		
		Raw Data ($T > 20$ s)	Corrected (*Woodhouse*)	PREM	HVZ	LVZ
				(*With Ellipticity*)		
2	Loyalty I. to Mid-East	8.51	8.47	8.55	8.42	8.73
3b	Tonga to Mid-East	8.50	8.47	8.56	8.40	8.75
4b	Tonga to Mid-East	8.46	8.46	8.55	8.44	8.74
7	Tonga to Mid-East	8.50	8.46	8.58	8.45	8.71
3a	Tonga to N.America	8.46	8.43	8.54	8.41	8.75
4a	Tonga to N.America	8.34	8.30	8.53	8.38	8.71
8	Tonga to N.America	8.46	8.42	8.55	8.38	8.73
6	Kuril Tr. to Americas	8.34	8.33	8.54	8.41	8.73
9	Honshu to Americas	8.33	8.30	8.57	8.43	8.76
10	Honshu to Americas	8.31	8.31	8.58	8.42	8.77
5	Burma to N.America	8.56	8.50	8.52	8.36	8.68
1	New Guinea to Europe	8.61	8.59	8.52	8.42	8.73

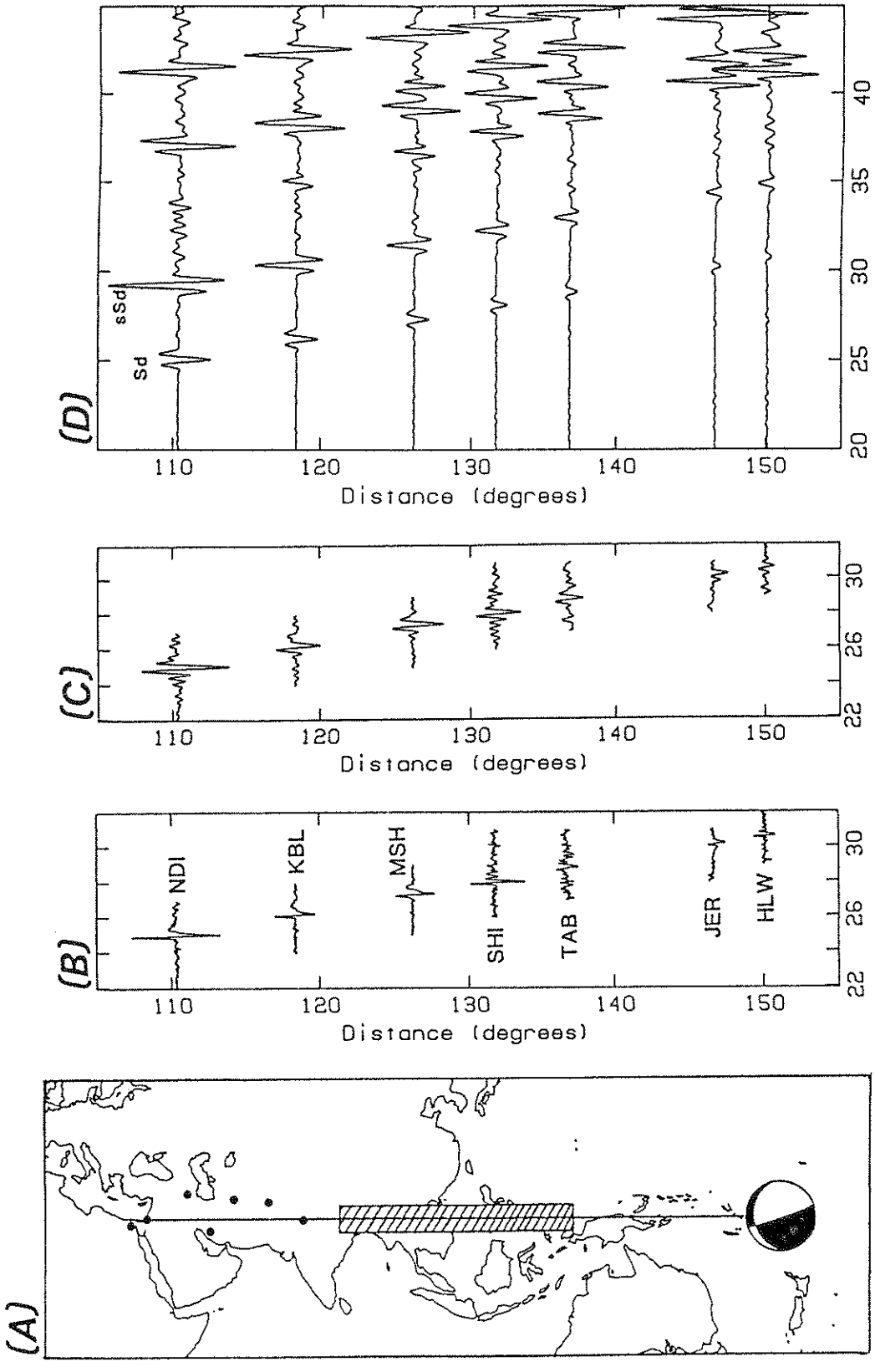

Fig. 2. Profiles for Event 4b to Asian and Mid-Eastern stations. (A) shows the path to the stations in relation to the focal mechanism and the region of CMB sampled (hatched). (B) and (C) show the *Sd* data before and after low-pass filtering at a cut-off frequency of 0.05 Hz. Note the amount of high-frequency energy still present out at 150°, in concurrence with observations of past studies [*Bolt et al.*, 1970]. (D) displays the PREM synthetic SH records from normal mode summation. In each case the apparent ray parameter corresponds to the linear trend through the *Sd* pulses.

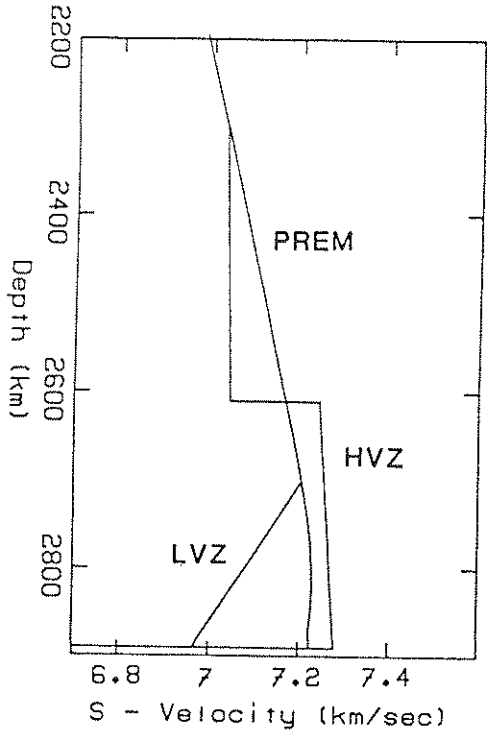

Fig. 3. The three D" SH-velocity structures used in the calculation of normal mode excitation functions for the generation of synthetic seismograms. The high-velocity model (HVZ) is in the style of the SLHO structure of *Lay and Helmberger* [1983*a*], and the low-velocity zone is modeled after M2 of *Mula and Müller* [1980].

zone of lower velocity that lies above it, so that the vertical travel-time of *ScS* will remain unchanged.

The LVZ, styled after model M2 of Mula and Müller [1980], is typical of low-velocity models in that its shear velocity reaches a maximum at the top of D" and decreases linearly with depth down to the CMB. At a radius of 3671 km the shear velocity reaches its maximum with $\beta = 7.2061$ km/s, and it decreases with a gradient of -1.26×10^{-3} s^{-1} down to a value of 6.965 km/s at the CMB. This is a modest relative (similar in structure but with a less pronounced negative velocity gradient) of several LVZ models previously presented, such as ANU2 of Hales and Roberts [1970] and that of Bolt [1972].

Cross-Correlation and Observations

The slownesses of both the *Sd* data and synthetics were determined using the cross-correlation method used by Okal and Geller [1979]. Since the data were filtered above 0.05 Hz and corrected for upper mantle heterogeneity, a comparison between the apparent ray parameters of data and synthetics is an appropriate means of testing the validity of our velocity models. The cross-correlation method, finding the best-fit linear trend between the *Sd* arrivals along a given path, involves isolating the *Sd* pulses, normalizing the signal energy of each pulse to unity and computing the cross-correlation functions $y_i \oplus y_j$ between the signals. The best-fitting slowness, p, corresponds to a maximum in the cross-correlation coefficient, F, determined by

$$F = \sum_i \sum_j y_i(t - p \cdot \Delta_i) \oplus y_j(t - p \cdot \Delta_j) \qquad (2)$$

Figure 4 shows the cross-correlation function $F(p)$ for the profile shown on Figure 2, and for the corresponding synthetics. Those paths which did not yield sharp and unitary peaks in the function $F(p)$ were discarded.

Previous studies of *Sd* waves have used visual picking methods in the determination of the slowness, choosing either the onsets [Bolt and Niazi, 1984] or peak deflections [Mula and Müller, 1980] of the arrivals, and had no means of correcting for the wave-forms changing due to the rapid high frequency decay. These methods would be very inappropriate for our study, with an absence of energy for periods $T < 20$ s in our pulses, but while the cross-correlation technique is also susceptible to bias from wave-form distortion, this distortion will appear in both data and synthetics and is therefore not problematic.

In all cases except Event 5, a tapered window was applied to isolate the *Sd* pulse before cross-correlation. For Event 5 (the Burma event and the shallowest earthquake used) the surface reflected *sSd* arrivals were so close to the *Sd* pulses that, with the absence of high frequencies, the two were distinct but inseparable. Therefore, the cross-correlated windows in these cases contained both signals, but given similar azimuths and take-off angles, the relative amplitudes and differential travel times between *Sd* and *sSd* arrivals should be the same at all stations and so should cause no bias in the calculated slowness.

Table 3 shows the slownesses for the paths used in our study. The first column is for the filtered data and the next includes the upper mantle corrections. It can clearly be seen that the addition of the heterogeneity corrections changes the slownesses by up to 0.06 s/°. In the tomographic model of Woodhouse [personal communication, 1987] we do see strong upper mantle velocity anomalies due to continent vs. ocean differences. Since all our stations are in continental regimes, we see a strong bias toward negative (fast) travel-time anomalies in our arrivals, but would have seen a greater variation in anomalies if we had used data from oceanic island stations, which tend to show a positive bias in travel times.

The last three columns of Table 3 show the synthetic slownesses from the three velocity models, with the ellipticity correction included. The effect of ellipticity varies depending upon the orientations of the profile path. For the two Honshu events this correction averaged +0.03 s/° among the three models, but was negligible for the Tonga profiles.

The variation in ray parameter due to the variable wave form frequency content from the unique juxtapositions of stations can be seen in the spherical model synthetics, which would otherwise yield identical slownesses for a given velocity model. For spherical PREM, which has the least vertical variance in D", the range in synthetic slownesses is 0.06 s/°, but for the other two models this range is 0.09 s/°, possibly due to their more complex structures. Add to this the corrections just mentioned and it is clear that in examining the path slownesses it is important not to attach significance to the individual values for the path-corrected data, but rather to their differentiation from the synthetic slownesses.

Figure 5 shows these comparisons as a function of the geographic region sampled at the CMB. "Average" shading is for slownesses between those of the PREM and HVZ models; "slow" implies velocities slower than PREM; "fast" implies velocities faster than our HVZ model. The four Tonga to Mid-East paths, sampling the CMB under the Western Pacific and Southeast Asia, all imply velocities close to the HVZ model but still possibly con-

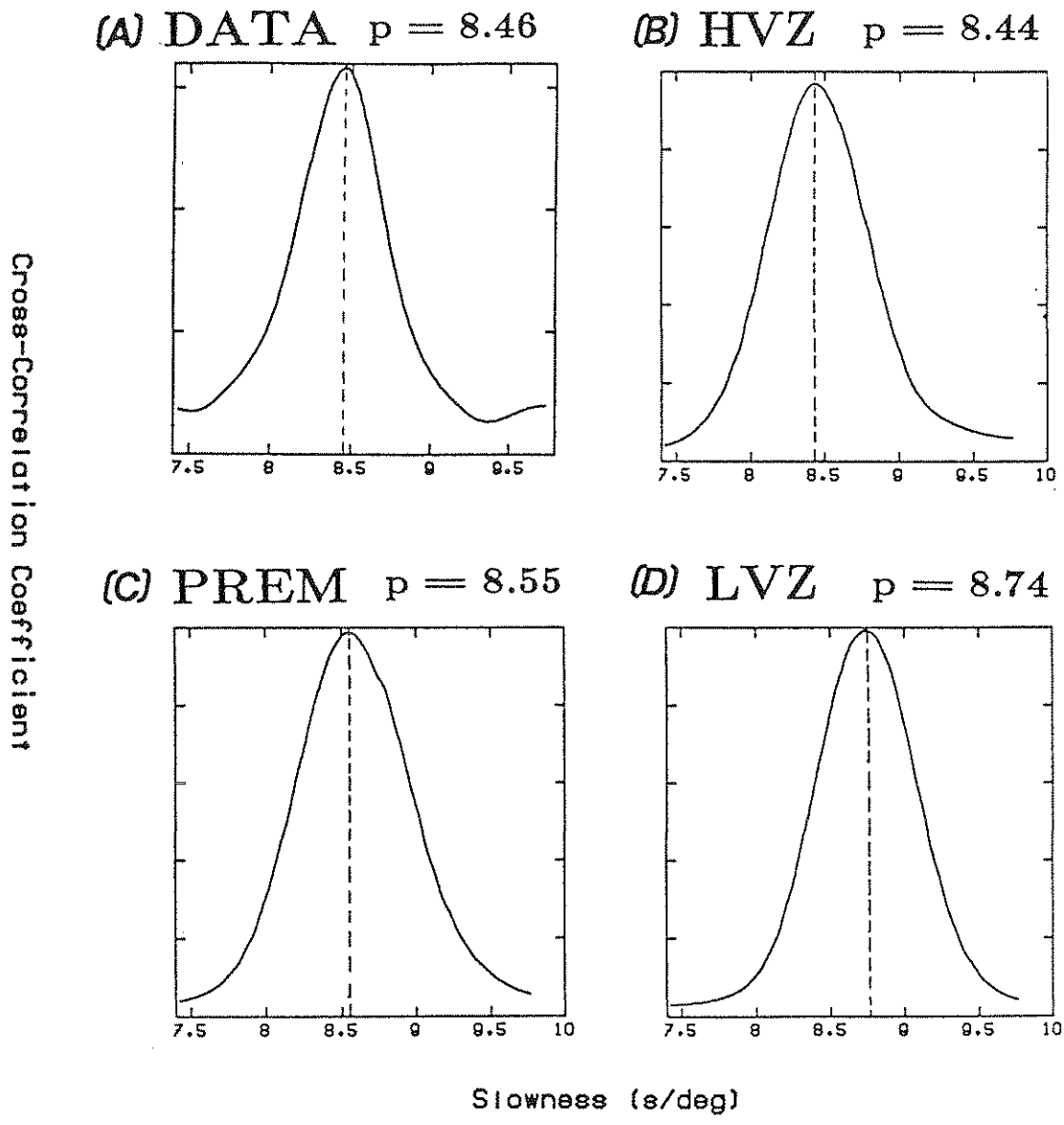

Fig. 4. Plots of the cross-correlation functions for the Event 4b profile. In (A), the peak represents the best-fitting apparent ray parameter through the filtered data arrivals (not corrected for upper mantle heterogeneity), and the following plots show the apparent slownesses through the synthetic *Sd* phases.

sistent with PREM. The three Tonga to North America paths suggest velocities even closer to our HVZ structure. The slowness for the Burma to North America path is consistent with that of the PREM synthetics.

All three Japan to America paths, however, show strikingly fast velocities, even faster than for our HVZ model. It is interesting to compare the geography of these results to that of Lay and Helmberger [1983b]. Because these authors' study is conducted at shorter distances, it is not possible to duplicate exactly their sampling. Nevertheless, their proposed area of high-velocity at the CMB, along the path from the Sea of Okhotsk to North America, falls in the immediate vicinity of our zone of high velocity (from Honshu and the Kuriles) to North and South America. Our HVZ was based on theirs in its structure but was also designed as a perturbation of PREM, maintaining *ScS* travel times. The Lay and Helmberger SLHO high-velocity zone had D" velocities in excess of 7.32 km/s (ours reached 7.28 km/s) and so would be more appropriate for our results than the HVZ we tested here. We do not have comparable coverage of their other region of high velocities (Argentina to North America).

The presence of a low-velocity zone was seen in only one region, the CMB under Siberia from our New Guinea to Europe profile. Even here, however, the slowness was only in between our PREM and LVZ models. Unfortunately, due to the paucity of stations in the Southern Hemisphere, we have no coverage of the CMB below the equator.

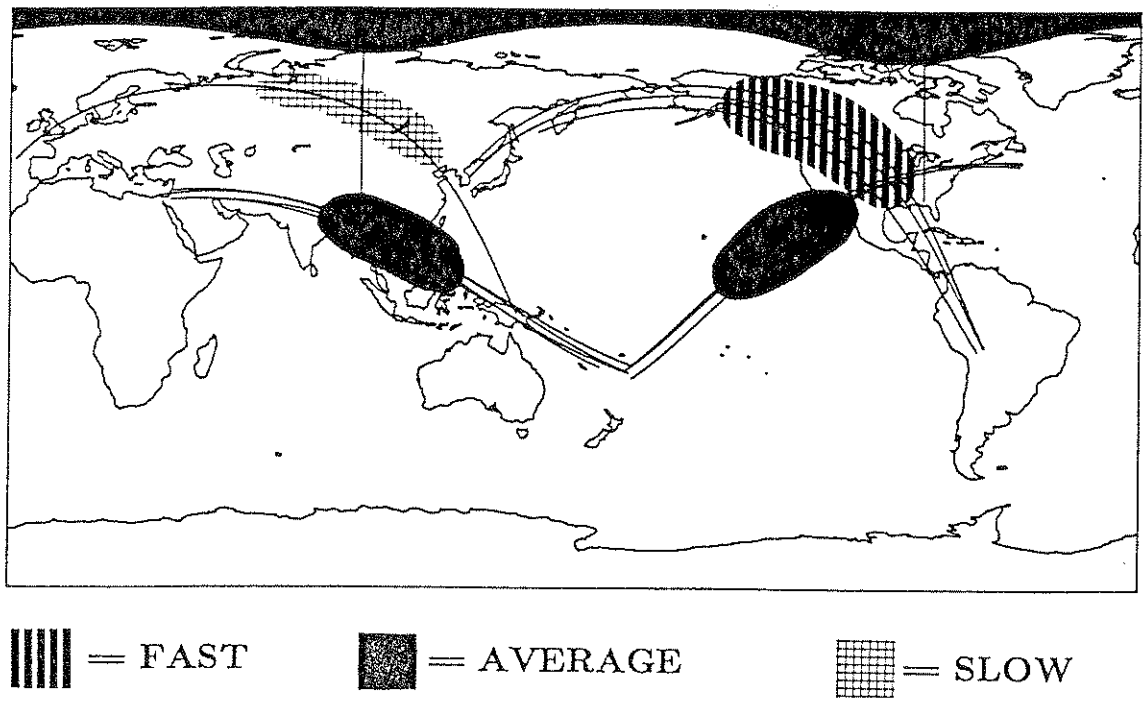

Fig. 5. Velocities in D" relative to the average of our data, which is slightly faster than for PREM. Solid lines represent average source-to-station great circle paths for the data profiles.

Conclusions

We find strong evidence for lateral heterogeneity in the velocity structure of the D" region at the base of the mantle. The use of diffracted SH waves is a powerful tool in examining this region, but considerations due to event depth and source parameters, station azimuth and location, ellipticity and slowness-determination techniques must first be taken into account. Both the ellipticity and upper mantle heterogeneity corrections can be significant for particular path profiles, and should be incorporated into future *Sd* ray parameter studies. In addition, inherent biases in the apparent ray parameter prevent a direct conversion into mantle velocities, but through comparison with synthetic seismograms generated through normal mode summation, we have been able to identify the appropriateness of different shear velocity models at different regions along the CMB. We find one region in D" that would be adequately modeled with a low-velocity perturbation to PREM (though not of the magnitude proposed by many other LVZ models), three regions that would be well represented by high-velocity perturbations to PREM, and one, in agreement with the results of Lay and Helmberger [1983b], that implies the presence of a very pronounced high-velocity zone. If high-velocity zones in D" were the result of the sinking of colder convected mantle, in the manner of Olson et al. [1987], and if full-mantle convection occurred, then the CMB directly below the Northern Pacific Ocean trenches, where oceanic lithosphere has continued to be subducted at a fast rate, would be a logical location.

Acknowledgements. We thank John Woodhouse for giving us a copy of his unpublished full-mantle 3-D shear wave velocity model, and Margie Yamasaki and the Lamont-Doherty Observatory for use of the seismology film chip library. This research was supported by NSF under grant EAR-84-5040.

References

Aki, K., and P. G. Richards, *Quantitative Seismology*, W. H. Freeman, San Francisco, 932 pp., 1980.

Bolt, B. A., The density distribution near the base of the mantle and near the Earth's center, *Phys. Earth Planet. Int., 5,* 301-311, 1972.

Bolt, B. A., N. Mansour, and M. R. Somerville, Diffracted ScS and shear velocity at the core boundary, *Geophys. J. R. astr. Soc., 19,* 299-305, 1970.

Bolt, B. A., and M. Niazi, S velocities in D" from diffracted SH-waves at the core boundary, *Geophys. J. R. astron. Soc., 79,* 825-834, 1984.

Chapman, C. H., and R. A. Phinney, Diffracted seismic signals and their numerical resolution, *Meth. Comput. Phys., 12,* 165-230, 1972.

Clayton, R. W., and R. P. Comer, A tomographic analysis of mantle heterogeneities from body wave travel time data, *Eos, Trans. Amer. Geophys. Un., 64,* 776, 1983 [abstract].

Cleary, J. R., The S velocity at the core-mantle boundary from observations of diffracted S, *Bull. seism. Soc. Am., 59,* 1399-1405, 1969.

Cleary, J. R., The D" region, *Phys. Earth Planet. Int., 30,* 13-27, 1974.

Cormier, V. F., Slab diffracted S waves, *Eos, Trans. Amer. Geophys. Un., 68,* 16, 1987 [abstract].

Dahlen, F. A., The normal modes of a rotating, elliptical Earth, *Geophys. J. R. Astron. Soc., 16,* 329-367,1968.

Dahlen, F. A., The correction of great circular surface wave phase velocity measurements for the rotation and ellipticity of the Earth, *J. Geophys. Res., 80,* 4895-4903, 1975.

Dahlen, F. A., and R. V. Sailor, Rotational and elliptical splitting of the free oscillations of the Earth, *Geophys. J. R. Astr. Soc., 58,* 609-623, 1979.

oornbos, D. J., and J. C. Mondt, Attenuation of *P* and *S* waves diffracted around the core, *Geophys. J. R. astr. Soc., 57,* 353-379, 1979.

Doornbos, D. J., and J. C. Mondt, The interaction of elastic waves with a solid-liquid interface, with applications to the core-mantle boundary, *Pageoph, 118,* 1293-1309, 1980.

Dziewonski, A. M., and D. L. Anderson, Preliminary reference Earth model, *Phys. Earth Planet. Int., 25,* 297-356, 1981.

Giardini, D., Systematic analysis of deep seismicity: 200 centroid-moment tensor solutions for earthquakes between 1977 and 1980, *Geophys. J. R. astron. Soc., 77,* 883-911, 1984.

Gudmundsson, O., R. W. Clayton, and D. L. Anderson, CMB topography from ISC *PcP* travel times, *Eos, Trans. Amer. Geophys. Un., 67,* 1100, 1987 [abstract].

Haddon, R. A. W., and G. R. Buchbinder, Wave propagation effects and the Earth's structure in the lower mantle, *Geophys. Res. Letts., 13,* 1489-1492, 1986.

Hales, A. L., and J. L. Roberts, Shear velocities in the lower mantle and the radius of the core, *Bull. Seismol. Soc. Am., 60,* 1427-1436, 1970.

Isacks, B., and P. Molnar, Distribution of stresses in the descending lithosphere from a global survey of focal mechanism solutions of mantle earthquakes, *Rev. Geophys. Space Phys., 9,* 103-174, 1971.

Jeanloz, R., and F. M. Richter, Convection, composition, and the thermal state of the lower mantle, *J. Geophys. Res., 84,* 5497-5504, 1979.

Jordan, T. H., and K. C. Creager, Chemical boundary layers of the mantle and core, *Eos, Trans. Amer. Geophys. Un., 68,* 1494-1495, 1987 [abstract].

Kanamori, H., and J. J. Cipar, Focal process of the great Chilean earthquake, *Phys. Earth Planet. Int., 9,* 128-136, 1974.

Kanamori, H., and G. S. Stewart, Mode of the strain release along the Gibbs Fracture Zone, Mid-Atlantic Ridge, *Phys. Earth Planet. Int., 11,* 312-332, 1976.

Lay, T., Evidence of a lower mantle shear velocity discontinuity in *S* and *sS* phases, *Geophys. Res. Letts., 13,* 1493-1496, 1986.

Lay, T., and D. V. Helmberger, A lower mantle S-wave triplication and the velocity structure of D", *Geophys. J. R. astr. Soc., 75,* 799-837, 1983*a*.

Lay, T., and D. V. Helmberger, The shear-wave velocity gradient at the base of the mantle, *J. Geophys. Res., 88,* 8160-8170, 1983*b*.

Mitchell, B. J., and D. V. Helmberger, Shear velocities at the base of the mantle from observations of S and ScS, *J. Geophys. Res., 78,* 6009-6027, 1973.

Mondt, J. C., SH waves: theory and observations for epicentral distances greater than 90 degrees, *Phys. Earth Planet. Int., 15,* 46-59, 1977.

Mula, A. H., Amplitudes of diffracted long-period P and S waves and the velocities and Q structure at the base of the mantle, *J. Geophys. Res., 86,* 4999-5011, 1981.

Mula, A. H., and G. Müller, Ray parameters of diffracted long period P and S waves and the velocities at the base of the mantle, *Pure Appl. Geophys., 118,* 1270-1290, 1980.

Okal, E. A., I. Application of normal mode theory to seismic source and structure problems; II. Seismic investigations of upper mantle lateral heterogeneity, *Ph.D. Thesis,* California Institute of Technology, 249 pp., Pasadena, 1978.

Okal, E. A., and R. J. Geller, Shear-wave velocity at the base of the mantle from profiles of diffracted SH waves, *Bull. Seismol. Soc. Am., 69,* 1039-1053, 1979.

Olson, P., G. Schubert, and C. Anderson, Plume formation in the D" layer and roughness on the core-mantle boundary, *Proc. XIXth Gen. Assemb. Intl. Un. Geod. Geophys.,* Vancouver, B. C., *V.1,* 6, 1987 [abstract].

Schlittenhardt, J., J. Schweitzer, and G. Müller, Evidence against a discontinuity at the top of D", *Geophys. J. Roy. astr. Soc., 81,* 295-306, 1985.

Tandon, A. N., and H. N. Srivastava, Fault plane solutions as related to known geological faults in and near India, *Ann. Geofis., 28,* 13-27, 1975.

Tanimoto, T., The three-dimensional shear wave structure in the mantle by overtone waveform inversion - I. Radial seismogram inversion, *Geophys. J. R. astr. Soc., 89,* 713-740, 1987.

Woodhouse, J. H., and F. A. Dahlen, The effect of a general aspherical perturbation on the free oscillations of the Earth, *Geophys. J. R. astr. Soc., 53,* 335-354, 1978.

Woodhouse, J. H., and A. M. Dziewonski, Mapping the upper mantle: Three-dimensional modeling of Earth structure by inversion of seismic waveforms, *J. Geophys. Res., 89,* 5953-5986, 1984.

Woodhouse, J. H., and A. M. Dziewonski, Models of the upper and lower mantle from waveforms of mantle waves and body waves, *Eos, Trans. Amer. Geophys. Un., 68,* 356-357, 1987 [abstract].